

Constraining the high-density behavior of the nuclear symmetry energy with the tidal polarizability of neutron stars

F. J. Fattoyev,^{1,2,*} J. Carvajal,^{1,3,†} W. G. Newton,^{1,‡} and Bao-An Li^{1,4,§}¹*Department of Physics and Astronomy, Texas A&M University–Commerces, Commerces, Texas 75429-3011, USA*²*Institute of Nuclear Physics, Tashkent 100214, Uzbekistan*³*Miami Dade College, 10525 SW 42nd TERR, Miami, Florida 33165, USA*⁴*Department of Applied Physics, Xian Jiao Tong University, Xian 710049, China*

(Received 11 October 2012; revised manuscript received 10 January 2013; published 31 January 2013)

Using a set of model equations of state satisfying the latest constraints from both terrestrial nuclear experiments and astrophysical observations, as well as state-of-the-art nuclear many-body calculations of the pure neutron matter equation of state, the tidal polarizability of canonical neutron stars in coalescing binaries is found to be a very sensitive probe of the high-density behavior of nuclear symmetry energy, which is among the most uncertain properties of dense neutron-rich nucleonic matter. Moreover, it changes less than $\pm 10\%$ by varying various properties of symmetric nuclear matter and symmetry energy around the saturation density within their respective ranges of remaining uncertainty.

DOI: [10.1103/PhysRevC.87.015806](https://doi.org/10.1103/PhysRevC.87.015806)

PACS number(s): 26.60.Kp, 21.65.Mn, 04.40.Dg

I. INTRODUCTION

Understanding the nature of neutron-rich nucleonic matter is a major thrust of current research in both nuclear physics and astrophysics [1]. To realize this goal, many experiments and observations are being carried out or proposed using a wide variety of advanced new facilities, such as Facilities for Rare Isotope Beams (FRIB), x-ray satellites, and gravitational wave (GW) detectors. Most critical to interpreting results of these experiments and observations is the equation of state (EOS) of neutron-rich nucleonic matter, i.e., $E(\rho, \alpha) = E_0(\rho) + S(\rho)\alpha^2 + \mathcal{O}(\alpha^4)$, where $E(\rho, \alpha)$ and $E_0(\rho)$ are the specific energy in asymmetric nuclear matter of isospin asymmetry $\alpha = (\rho_n - \rho_p)/\rho$ and symmetric nuclear matter (SNM), respectively, and $S(\rho)$ is the symmetry energy encoding the energy cost of converting all protons in SNM to neutrons. Thanks to the continuing efforts of both the nuclear physics and astrophysics communities over several decades, the EOS of SNM around the saturation density ρ_0 has been well constrained. Moreover, combining information from studying the collective flow and kaon production in relativistic heavy-ion collisions in several terrestrial nuclear physics laboratories [2], and the very recent discovery of the maximum mass of neutron stars [3], the EOS of SNM has been limited in a relatively small range up to about $4.5\rho_0$. The symmetry energy $S(\rho)$ is a vital ingredient in describing the structure of rare isotopes and their reaction mechanisms. It also determines uniquely the proton fraction and thus the cooling mechanism, appearance of hyperons, and possible kaon condensation in neutron stars. Moreover, it affects significantly the structure, such as the radii, moment

of inertia and the core-crust transition density, as well as the frequencies and damping times of various oscillation modes of neutron stars; see, e.g., Refs. [4,5] for reviews. Intensive efforts devoted to constraining $S(\rho)$ using various approaches have recently led to a close convergence around $S(\rho_0) \approx 30$ MeV and its density slope $L \equiv 3\rho_0(dS(\rho)/d\rho)_{\rho_0} \approx 50$ MeV with a few exceptions, although the error bars for L from different approaches may vary broadly [6–12]. On the other hand, the high-density behavior of $S(\rho)$ remains very uncertain despite its importance to understanding what happens in the core of neutron stars [13–17] and in reactions with high energy radioactive beams [18]. The predictions for the high-density behavior of the symmetry energy from all varieties of nuclear models diverge dramatically [19–21], with some models predicting very stiff symmetry energies that increase continuously with density [21–26], and others predicting relatively soft ones, or an $S(\rho)$ that first increases with density, then saturates and starts decreasing with increasing density [19,27–41]. These uncertainties can be traced to our poor knowledge about the isospin dependence of the strong interaction in the dense neutron-rich medium, particularly the spin-isospin dependence of three-body and many-body forces, the short-range behavior of the nuclear tensor force, and the isospin dependence of nucleon-nucleon correlations in the dense medium; see, e.g., Refs. [42,43]. Little experimental progress has been made in constraining the high-density $S(\rho)$, partially because of the lack of sensitive probes. While several observables have been proposed [18] and some indications of the high-density $S(\rho)$ have been reported recently [44,45], conclusions based on terrestrial nuclear experiments remain controversial [46]. To our best knowledge, the only astrophysical probe for high-density $S(\rho)$ proposed so far is the late-time neutrino signal from a core collapse supernova [47]. In this article, we show that the tidal polarizability of canonical neutron stars in coalescing binaries is a very sensitive probe of the high-density behavior of the nuclear symmetry energy independent of the remaining uncertainties of the SNM EOS and $S(\rho)$ near saturation density.

*Farrooh.Fattoyev@tamuc.edu

†Jose.Carvajal002@mymdc.net

‡William.Newton@tamuc.edu

§Bao-An.Li@tamuc.edu

The paper has been organized as follows. In Sec. II we provide the background material necessary to compute the stellar structure and tidal polarizability. In Sec. III we discuss current theoretical, experimental, and observational constraints on the nuclear matter EOS, and prepare several parametrizations that will be used to compute the EOS of the stellar material. We note that these parametrizations not only reproduce various experimentally measured properties of finite nuclei, but are also systematically varied within the available constraints such that they cover the full constraint region in their predictions for the EOS at both low and high densities. In Sec. IV we present results for various neutron-star properties, including the tidal polarizability of a canonical neutron star, and discuss their sensitivity to the EOS. Finally, Sec. V summarizes our concluding remarks and suggestions for future work.

II. STELLAR STRUCTURE AND TIDAL POLARIZABILITY

Coalescing binary neutron stars are among the most promising sources of gravitational waves. One of the most important features of binary mergers is the tidal deformation neutron stars undergo as they approach each other prior to merger, the strength of which can give us precious information about the neutron-star matter EOS [48–59]. At the early stage of an inspiral, tidal effects may be effectively described through the tidal polarizability parameter λ [48,51–53] defined via $Q_{ij} = -\lambda \mathcal{E}_{ij}$, where Q_{ij} is the induced quadrupole moment of a star in binary, and \mathcal{E}_{ij} is the static external tidal field of the companion star. The tidal polarizability can be expressed in terms of the dimensionless tidal Love number k_2 and the neutron star radius R as $\lambda = 2k_2 R^5 / (3G)$. The tidal Love number k_2 is found using the following expression [49,54]:

$$k_2 = \frac{1}{20} \left(\frac{R_s}{R} \right)^5 \left(1 - \frac{R_s}{R} \right)^2 \left[2 - y_R + (y_R - 1) \frac{R_s}{R} \right] \times \left\{ \frac{R_s}{R} \left(6 - 3y_R + \frac{3R_s}{2R} (5y_R - 8) + \frac{1}{4} \left(\frac{R_s}{R} \right)^2 \right) \times \left[26 - 22y_R + \left(\frac{R_s}{R} \right) (3y_R - 2) + \left(\frac{R_s}{R} \right)^2 (1 + y_R) \right] + 3 \left(1 - \frac{R_s}{R} \right)^2 \left[2 - y_R + (y_R - 1) \frac{R_s}{R} \right] \times \ln \left(1 - \frac{R_s}{R} \right) \right\}^{-1}, \quad (1)$$

where $R_s \equiv 2M$ is the Schwarzschild radius of the star, and $y_R \equiv y(R)$ can be calculated by solving the following first-order differential equation:

$$r \frac{dy(r)}{dr} + y(r)^2 + y(r)F(r) + r^2 Q(r) = 0, \quad (2)$$

with

$$F(r) = \frac{r - 4\pi r^3 [\mathcal{E}(r) - P(r)]}{r - 2M(r)}, \quad (3)$$

$$Q(r) = \frac{4\pi r (5\mathcal{E}(r) + 9P(r) + \frac{\mathcal{E}(r)+P(r)}{\partial P(r)/\partial \mathcal{E}(r)} - \frac{6}{4\pi r^2})}{r - 2M(r)} - 4 \left[\frac{M(r) + 4\pi r^3 P(r)}{r^2 (1 - 2M(r)/r)} \right]^2. \quad (4)$$

Eq. (2) must be integrated together with the Tolman-Oppenheimer-Volkoff (TOV) equation. That is,

$$\frac{dP(r)}{dr} = - \frac{(\mathcal{E}(r) + P(r))(M(r) + 4\pi r^3 P(r))}{r^2 (1 - 2M(r)/r)}, \quad (5)$$

$$\frac{dM(r)}{dr} = 4\pi r^2 \mathcal{E}(r). \quad (6)$$

Given the boundary conditions in terms of $y(0) = 2$, $P(0) = P_c$, and $M(0) = 0$, the tidal Love number can be obtained once an EOS is supplied. Previous studies have used both polytropic EOSs and several popular nuclear EOSs available in the literature [48–59]. While other particles may be present, for the purpose of this work, it is sufficient to assume that neutron stars consist of only neutrons (n), protons (p), electrons (e), and muons (μ) in β equilibrium.

III. CONSTRAINED EOS OF NEUTRON-RICH NUCLEAR MATTER

We use two classes of nuclear EOSs within the relativistic mean field (RMF) model and the Skyrme Hartree-Fock (SHF) approach. The RMF model traditionally includes an isodoublet nucleon field (ψ) interacting via the exchange of the scalar-isoscalar σ meson (ϕ), the vector-isoscalar ω meson (V^μ), the vector-isovector ρ meson (\mathbf{b}^μ), and the photon (A^μ) [60–62]. The full Lagrangian density for such a model can be written as

$$\mathcal{L} = \bar{\psi} \left[\gamma^\mu \left(i\partial_\mu - g_\nu V_\nu - \frac{g_\rho}{2} \boldsymbol{\tau} \cdot \mathbf{b}_\mu - \frac{e}{2} (1 + \tau_3) A_\mu \right) - (M - g_s \phi) \right] \psi + \frac{1}{2} \partial_\mu \phi \partial^\mu \phi - \frac{1}{2} m_s^2 \phi^2 - \frac{1}{4} V^{\mu\nu} V_{\mu\nu} + \frac{1}{2} m_v^2 V^\mu V_\mu - \frac{1}{4} \mathbf{b}^{\mu\nu} \cdot \mathbf{b}_{\mu\nu} + \frac{1}{2} m_\rho^2 \mathbf{b}^\mu \cdot \mathbf{b}_\mu - \frac{1}{4} F^{\mu\nu} F_{\mu\nu} - U(\phi, V_\mu, \mathbf{b}_\mu), \quad (7)$$

where $V_{\mu\nu} \equiv \partial_\mu V_\nu - \partial_\nu V_\mu$, $\mathbf{b}_{\mu\nu} \equiv \partial_\mu \mathbf{b}_\nu - \partial_\nu \mathbf{b}_\mu$, and $F_{\mu\nu} \equiv \partial_\mu A_\nu - \partial_\nu A_\mu$ are the isoscalar, isovector, and electromagnetic field tensors, respectively. The four constants represent the nucleon mass M and meson masses m_s , m_v , m_ρ and may be treated as empirical parameters. In addition to the standard Yukawa interactions, the Lagrangian is supplemented with an effective potential $U(\phi, V_\mu, \mathbf{b}_\mu)$ that consists of nonlinear meson interactions that simulates the complicated dynamics encoded in a handful of accurately calibrated model parameters. In this work we use the following form of the effective potential [63]:

$$U(\phi, V^\mu, \mathbf{b}^\mu) = \frac{\kappa}{3!} (g_s \phi)^3 + \frac{\lambda}{4!} (g_s \phi)^4 - \frac{\zeta}{4!} g_v^4 (V_\mu V^\mu)^2 - \Lambda_v g_\rho^2 \mathbf{b}_\mu \cdot \mathbf{b}^\mu g_v^2 V_\nu V^\nu. \quad (8)$$

Note that, if one would like to consider all nonlinear terms to the fourth order in meson fields and also incorporate the seldom used scalar-isovector δ meson [64,65], then 15 additional parameters must be included in the Lagrangian above (1 Yukawa coupling and 14 meson self-interaction terms). Remarkably, using just a few model parameters and without invoking the scalar-isovector δ -meson interaction even to the lowest order with just a Yukawa coupling, it is possible to reproduce a host of ground-state properties of finite nuclei throughout the periodic table [66,67], the nuclear collective excitations, and neutron-star properties [24,63,68,69] with very high accuracy.

Following standard mean-field practices, the energy density of the system can be written as

$$\begin{aligned} \mathcal{E}(\rho, \alpha) = & \frac{1}{\pi^2} \int_0^{k_F^p} k^2 E_k^* dk + \frac{1}{\pi^2} \int_0^{k_F^n} k^2 E_k^* dk \\ & + g_v V_0 \rho + \frac{g_\rho}{2} b_0 \rho_3 + \frac{1}{2} m_s^2 \phi_0^2 + \frac{\kappa}{3!} (g_s \phi_0)^3 \\ & + \frac{\lambda}{4!} (g_s \phi_0)^4 - \frac{1}{2} m_v^2 V_0^2 - \frac{\zeta}{4!} (g_v V_0)^4 \\ & - \frac{1}{2} m_\rho^2 b_0^2 - \Lambda_v (g_v V_0)^2 (g_\rho b_0)^2, \end{aligned} \quad (9)$$

where $\alpha = -\rho_3/\rho$ is the isospin asymmetry, $\rho_3 \equiv \rho_p - \rho_n$ is the isovector baryon density, $E_k^* = \sqrt{k^2 + M^{*2}}$, $M^* = M - g_s \phi_0$ is the nucleon (Dirac) effective mass, and k_F^p (k_F^n) is the proton (neutron) Fermi momentum. Since the mean-field approximation is thermodynamically consistent, the pressure of the system at zero temperature may be obtained either from the energy-momentum tensor or from the energy density and its first derivative with respect to the density [60,61]. That is,

$$P(\rho, \alpha) = \rho \frac{\partial \mathcal{E}(\rho, \alpha)}{\partial \rho} - \mathcal{E}(\rho, \alpha).$$

All of the EOSs are adjusted to satisfy the following four conditions within their respective uncertain ranges: (1) reproducing the PNM EOS at sub-saturation densities predicted by the latest state-of-the-art microscopic nuclear many-body theories [28,70–75]; (2) predicting correctly saturation properties of symmetric nuclear matter, i.e., nucleon binding energy $B = -16 \pm 1$ MeV and incompressibility $K_0 = 230 \pm 20$ MeV [76,77], and nucleon (Dirac) effective mass $M_{D,0}^* = 0.61 \pm 0.03M$ [78] at saturation density $\rho_0 = 0.155 \pm 0.01$ fm $^{-3}$; (3) predicting a fiducial value of symmetry energy $S(2\rho_0/3) = 26 \pm 0.5$ MeV, $J \equiv S(\rho_0) = 31 \pm 2$ MeV, and the density slope of symmetry energy $L = 50 \pm 10$ MeV (See Ref. [12] and references therein); (4) passing through the terrestrial constraints on the EOS of SNM between $2\rho_0$ and $4.5\rho_0$ [2] and giving a maximum mass of neutron stars of about $2M_\odot$, assuming they are made of only the $npe\mu$ matter without considering other degrees of freedom or invoking any exotic mechanism [3,79].

To compare the RMF and SHF models on the same basis, we also create SHF parametrizations which give the same properties of nuclear matter at saturation as the RMF parametrizations, through the method of writing the Skyrme parameters as functions of macroscopic nuclear quantities

[80,81]. Note that several definitions of the nucleon effective mass exist in the literature [82]. In the RMF model the Dirac effective mass is defined through the scalar part of the nucleon self-energy in the Dirac equation. It is well known that, in order to reproduce the empirical spin-orbit couplings in finite nuclei, the Dirac effective mass at saturation density $M_{D,0}^*$ must lie in the range of $0.58 < M_{D,0}^*/M < 0.64$ [61,78,83–85]. While microscopic calculations based on realistic meson-exchange models for the nucleon-nucleon interaction suggest that the isovector δ -meson contribution to the scalar field may be very important [86,87], thus resulting in a sizable difference in the nucleon effective (Dirac) masses, we rely on a minimal model without the δ meson, which accurately reproduces binding energies and charge radii of doubly magic nuclei, and neutron-star properties [24,63,68,69]. This minimal model meets the requirements of our current study, which is to have two tunable parameters controlling the saturation density stiffness of the symmetry energy and the high-density stiffness of the SNM EOS, while still reproducing the minimal set of nuclear matter properties relevant for basic neutron star structure. Indeed, the inclusion of a δ meson in the RMF model gives rise to a stiff EOS of asymmetric nuclear matter at high densities [64,65], which in turn results in larger neutron star radii predictions that lie just at the edge of the range currently inferred from observation [8,79]. In our current minimal model, neglecting the effects of δ -meson contributions gives us identical nucleon effective masses for both SNM and PNM. On the other hand, the nonrelativistic effective mass parametrizes the momentum dependence of the single-particle potential, which is the result of a quadratic parametrization of the single-particle spectrum. It has been argued [88] that the so-called Lorentz mass M_L^* in SNM should be compared with the nonrelativistic effective mass extracted from analyses carried out in the framework of nonrelativistic optical and shell models. For consistency, at saturation density for SNM we choose the effective mass in the SHF model to be equal to the Lorentz mass in the RMF model. Moreover, since the effective masses in the RMF model used in this work are the same for both protons and neutrons, we set them equal in the equivalent SHF model too. As an example, two such EOSs obtained using the IU-FSU RMF model [69] and the SHF using the SkiIU-FSU parameter set [12] are shown in Fig. 1. By design, they both have the same EOS for SNM and PNM around and below ρ_0 . Thus, at subsaturation densities the values of $S(\rho)$ which is approximately the difference between the EOSs for PNM and SNM are almost identical for the two models. However, the values of $S(\rho)$ are significantly different above about $1.5\rho_0$ with the IU-FSU leading to a much stiffer $S(\rho)$ at high densities. More quantitatively, the $S(\rho)$ with IU-FSU is 40%–60% higher in the density range of $\rho/\rho_0 = 3$ –4 expected to be attained in the core of canonical neutron stars. In our previous study we showed that this is a generic feature of the models [12].

To test the sensitivity of the tidal polarizability to variations of properties of neutron-rich nuclear matter around ρ_0 within the constraints listed above, we build 17 RMF parametrizations by systematically varying the values of K_0 , M_0^* , L , and the ζ parameter of the RMF model that controls the omega-meson self-interactions [62] and subsequently the high-density component of the EOS of SNM. Besides the constraints listed

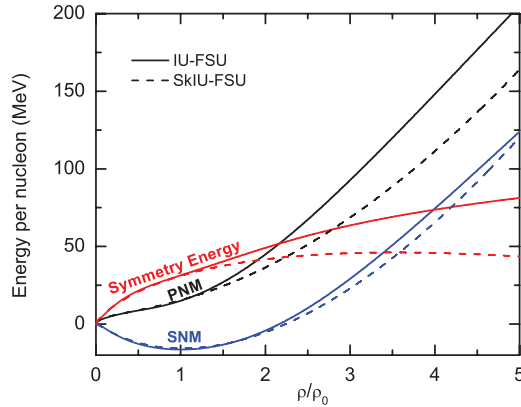


FIG. 1. (Color online) The EOS of SNM and PNM as well as the symmetry energy as a function of density obtained within the IU-FSU RMF model and the SHF approach using the SKIU-FSU parameter set.

above, all parameter sets can correctly reproduce the experimental values for the binding energy and charge radius of ^{208}Pb and the ground-state properties of other closed shell nuclei within 2% uncertainty [89]. As a reference for comparisons, we select $K_0 = 230$ MeV, $M_0^* = 0.61 M$, $L = 50$ MeV, and $\zeta = 0.025$ for our base model, which predicts $\rho_0 = 0.1524$ fm $^{-3}$, $B = -16.33$ MeV, and $J = 31.64$ MeV. The representative model EOSs for PNM at subsaturation densities and those for SNM at suprasaturation densities are compared with their constraints in Figs. 2 and 3, respectively. It is seen that the SKIU-FSU and all the RMF models with $42 < L < 58$ MeV can satisfy the PNM EOS constraint. Also, they can all satisfy simultaneously the high-density SNM EOS constraint with $0.02 < \zeta < 0.03$. Moreover, they all give a maximum mass for neutron stars between $1.94M_\odot$ and $2.07M_\odot$ and radii between 12.33 and 13.22 km for canonical neutron stars [69], consistent with existing observations [3,79,90].

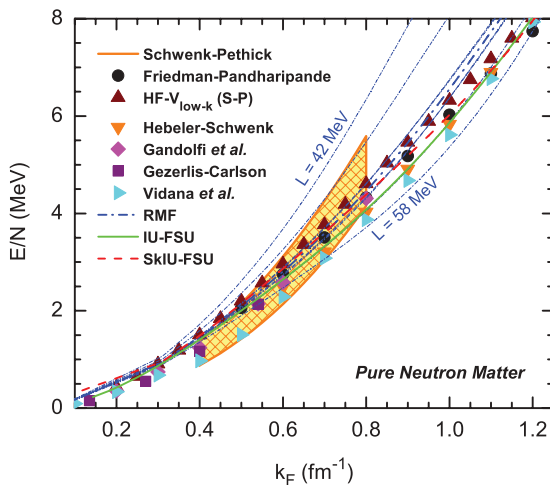


FIG. 2. (Color online) Energy per nucleon as a function of the Fermi momentum for PNM for selected models described in the text.

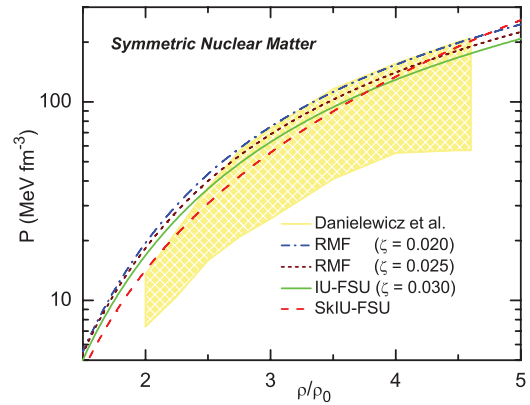


FIG. 3. (Color online) The pressure of SNM given as the function of baryon density. Here ρ_0 is the nuclear matter saturation density and the shaded area represents the EOS extracted from the analysis of Ref. [2].

IV. RESULTS AND DISCUSSIONS

First, we examine sensitivities of the tidal polarizability λ of a $1.4M_\odot$ neutron star to the variations of SNM properties and the slope of the symmetry energy around ρ_0 in Fig. 4 and Table I. The changes of λ relative to the values for our base RMF model are shown for the remaining RMF EOSs. It is very interesting to see that the tidal polarizability is rather insensitive to the variation of L within the constrained range, although it changes up to $\pm 10\%$ with K_0 , M^* , and ζ within their individual uncertain ranges. While the averaged mass is $M = 1.33 \pm 0.05M_\odot$, neutron stars in binaries have a broad mass distribution [91]. It is thus necessary to investigate the mass dependence of the tidal polarizability. Whereas what can be measured for a neutron star binary of mass M_1 and M_2 is

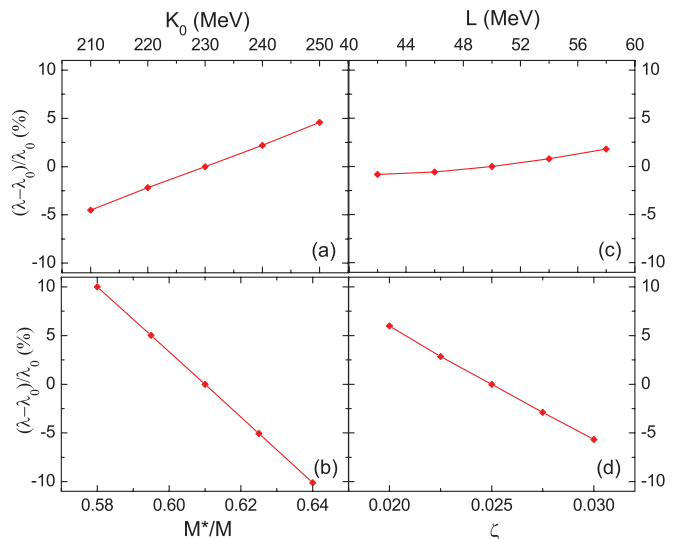


FIG. 4. (Color online) Percentage changes in the tidal polarizability of a 1.4 solar mass neutron star by individually varying properties of nuclear matter K_0 (a), M^* (b), L (c), and the ζ parameter (d) of the RMF model with respect to the value using the base model.

TABLE I. Predictions for the properties of a 1.4 solar-mass neutron star using the 17 EOSs considered in this paper. We systematically vary the properties of nuclear matter around our base parametrization (as discussed in the text) to create different EOSs as diverse as possible, but within the available theoretical, experimental, and observational constraints. The first column reports the name of the EOS with a particular nuclear property and/or ζ parameter indicated. The radii are in units of km, the tidal polarizability in $10^{36} \text{ cm}^2 \text{ g s}^2$.

EOS	R	M/R	k_2	λ	$\Delta\lambda/\lambda$
Base	12.88	0.1605	0.0879	3.115	
$K = 210 \text{ MeV}$	12.82	0.1612	0.0858	2.974	-4.52 %
$K = 220 \text{ MeV}$	12.85	0.1608	0.0869	3.046	-2.19 %
$K = 240 \text{ MeV}$	12.91	0.1602	0.0890	3.183	+2.21 %
$K = 250 \text{ MeV}$	12.94	0.1598	0.0900	3.258	+4.59 %
$M^* = 0.580M$	12.71	0.1626	0.1033	3.427	+10.01 %
$M^* = 0.595M$	12.83	0.1612	0.0943	3.271	+5.02 %
$M^* = 0.625M$	12.89	0.1604	0.0831	2.957	-5.06 %
$M^* = 0.640M$	12.88	0.1606	0.0792	2.800	-10.12 %
$L = 42 \text{ MeV}$	12.33	0.1677	0.1086	3.089	-0.83 %
$L = 46 \text{ MeV}$	12.64	0.1635	0.0960	3.096	-0.58 %
$L = 54 \text{ MeV}$	13.07	0.1582	0.0824	3.140	+0.80 %
$L = 58 \text{ MeV}$	13.22	0.1564	0.0787	3.170	+1.79 %
$\zeta = 0.0200$	13.01	0.1589	0.0885	3.302	+6.00 %
$\zeta = 0.0225$	12.94	0.1597	0.0882	3.204	+2.85 %
$\zeta = 0.0275$	12.81	0.1613	0.0876	3.025	-2.90 %
$\zeta = 0.0300$	12.75	0.1622	0.0873	2.938	-5.67 %

the mass-weighted tidal polarizability [53]

$$\tilde{\lambda} = \frac{1}{26} \left[\frac{M_1 + 12M_2}{M_1} \lambda_1 + \frac{M_2 + 12M_1}{M_2} \lambda_2 \right], \quad (10)$$

for the purpose of this study it is sufficient to consider binaries consisting of two neutron stars with equal masses. What can we learn from the tidal polarizability of light and massive neutron stars, respectively? Shown in Fig. 5 is the tidal polarizability λ

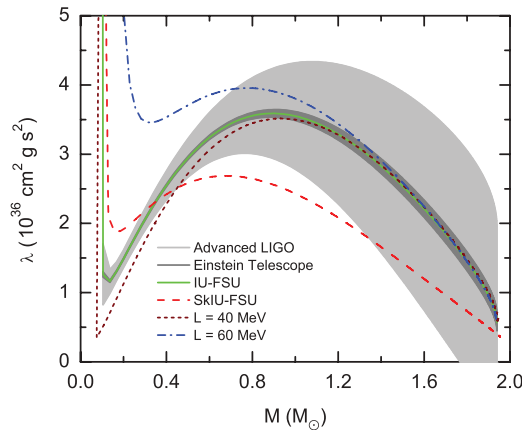


FIG. 5. (Color online) Tidal polarizability λ of a single neutron star as a function of neutron-star mass for a range of EOS that allow various stiffness of symmetry energies. A crude estimate of uncertainties in measuring λ for equal mass binaries at a distance of $D = 100 \text{ Mpc}$ is shown for the Advanced LIGO detector (shaded light-grey area) and the Einstein Telescope (shaded dark-grey area).

TABLE II. Predictions for the properties of a 1.4 solar-mass neutron star using the IU-FSU EOS with different density dependence of the symmetry energy. The slopes of the symmetry energy are in units of MeV, radii are in units of km, and the tidal polarizability in $10^{36} \text{ cm}^2 \text{ g s}^2$. The relative percentage error $\Delta\lambda/\lambda$ is calculated with respect to the original IU-FSU parametrization [69].

EOS	L	R	M/R	k_2	λ	$\Delta\lambda/\lambda$
IU-FSU-0	47.2	12.49	0.1655	0.0930	2.828	
IU-FSU-1	40.0	12.20	0.1695	0.1054	2.841	+0.46 %
IU-FSU-2	60.0	13.07	0.1581	0.0761	2.906	+2.76 %
SkIU-FSU	47.2	11.71	0.1765	0.0753	1.657	-41.41 %

as a function of neutron-star mass for a range of EOSs. Most interestingly, it is seen that the IU-FSU and SkIU-FSU models which are different only in their predictions for the nuclear symmetry energy above about $1.5\rho_0$, as shown in Fig. 1, lead to significantly different λ values in a broad mass range from $0.5M_\odot$ to $2M_\odot$. More quantitatively, a 41% change in λ from 2.828×10^{36} (IU-FSU) to 1.657×10^{36} (SkIU-FSU) is observed for a canonical neutron star of $1.4M_\odot$ (See Table II). For a comparison, we notice that this effect is as strong as the symmetry energy effect on the late-time neutrino flux from the cooling of proto-neutron stars [47]. Moreover, it is shown that the variation of L has a very small effect on the tidal polarizability λ of massive neutron stars, which is consistent with the results shown in Fig. 4. On the other hand, the L parameter affects significantly the tidal polarizability of neutron stars with $M \leq 1.2M_\odot$. These observations can be easily understood. From Eq. (1) the Love number k_2 is essentially determined by the compactness parameter M/R and the function $y(R)$. Both of them are obtained by integrating the EOS all the way from the core to the surface. Since the saturation density approximately corresponds to the central density of a $0.3M_\odot$ neutron star, one thus should expect only the Love number of low-mass neutron stars to be sensitive to the EOS around the saturation density. However, for canonical and more massive neutron stars, the central density is higher than $3\rho_0$ – $4\rho_0$, and therefore both the compactness M/R and $y(R)$ show stronger sensitivity to the variation of EOS at suprasaturation densities. Since all the EOSs for SNM at suprasaturation densities have already been constrained by the terrestrial nuclear physics data and required to give a maximum mass about $2M_\odot$ for neutron stars, the strongest effect on calculations of the tidal polarizability of massive neutron stars should therefore come from the high-density behavior of the symmetry energy.

It has been suggested that the Advanced LIGO-Virgo detector may potentially measure the tidal polarizability of binary neutron stars with a moderate accuracy. Are the existing or planned GW detectors sensitive enough to measure the predicted effects of high-density symmetry energy on the tidal polarizability? To answer this question, as an example we estimate uncertainties in measuring λ for equal-mass binaries at an optimally oriented distance of $D = 100 \text{ Mpc}$ [53,92] using the same approach as detailed in Refs. [53,59]. These are shown for the Advanced LIGO-Virgo detector (shaded light-grey area) and the Einstein Telescope (shaded dark-grey

area) in Fig. 5. It is seen that discerning between high-density symmetry energy behaviors is at the limit of the Advanced LIGO-Virgo detector's sensitivity for stars of mass $1.4M_{\odot}$ and below based on the currently estimated uncertainty, and it is possible that a rare but nearby binary system may be found and provide a much tighter constraint [53]. Nevertheless, measurements for binaries consisting of light neutron stars can still help further constrain the symmetry energy around the saturation density. On the other hand, it is noteworthy that the narrow uncertain range for the proposed Einstein Telescope will enable it to tightly constrain the symmetry energy especially at high densities.

V. CONCLUSIONS

Using the EOSs for neutron-rich nucleonic matter satisfying the latest constraints from both terrestrial nuclear experiments and astrophysical observations, as well as the state-of-the-art nuclear many-body calculations for PNM EOS, we found that

the tidal polarizability of canonical neutron stars starts in coalescing binaries is very sensitive to the high-density behavior of nuclear symmetry energy, but little affected by the variations of SNM EOS and symmetry energy around the saturation density within their remaining uncertainty ranges. Future measurements of the tidal polarizability of neutron stars using the forthcoming GW detectors, most notably the proposed Einstein Telescope, will help constrain stringently the high-density behavior of nuclear symmetry energy, and thus the nature of dense neutron-rich nucleonic matter.

ACKNOWLEDGMENTS

We would like to thank Dr. J. Piekarewicz and Dr. Jun Xu for various useful discussions. This work is supported in part by the National Aeronautics and Space Administration under Grant No. NNX11AC41G issued through the Science Mission Directorate, and the National Science Foundation under Grants No. PHY-0757839, No. PHY-1062613, and No. PHY-1068022.

-
- [1] The 2007 US NSAC Long Range Plan, <http://www.er.doe.gov/np/nsac/nsac.html>.
 - [2] P. Danielewicz, R. Lacey, and W. G. Lynch, *Science* **298**, 1592 (2002).
 - [3] P. B. Demorest, T. Pennucci, S. M. Ransom, M. S. E. Roberts, and J. W. T. Hessels, *Nature (London)* **467**, 1081 (2010).
 - [4] J. M. Lattimer and M. Prakash, *Phys. Rep.* **333**, 121 (2000).
 - [5] J. M. Lattimer and M. Prakash, *Science* **304**, 536 (2004).
 - [6] C. Xu, B.-A. Li, and L.-W. Chen, *Phys. Rev. C* **82**, 054607 (2010).
 - [7] W. G. Newton, M. Gearheart, and B.-A. Li, *Astrophys. J. Suppl.* **204**, 9 (2013).
 - [8] A. W. Steiner and S. Gandolfi, *Phys. Rev. Lett.* **108**, 081102 (2012).
 - [9] J. M. Lattimer and Y. Lim, [arXiv:1203.4286](https://arxiv.org/abs/1203.4286).
 - [10] M. Dutra, O. Lourenço, J. S. Sà Martins, A. Delfino, J. R. Stone, and P. D. Stevenson, *Phys. Rev. C* **85**, 035201 (2012).
 - [11] M. Tsang *et al.*, *Phys. Rev. C* **86**, 015803 (2012).
 - [12] F. J. Fattoyev, W. G. Newton, J. Xu, and B.-A. Li, *Phys. Rev. C* **86**, 025804 (2012).
 - [13] M. Kutschera, *Phys. Lett. B* **340**, 1 (1994).
 - [14] S. Kubis and M. Kutschera, *Acta Phys. Pol. B* **30**, 2747 (1999).
 - [15] S. Kubis and M. Kutschera, *Nucl. Phys. A* **720**, 189 (2003).
 - [16] D.-H. Wen, B.-A. Li, and L.-W. Chen, *Phys. Rev. Lett.* **103**, 211102 (2009).
 - [17] H. K. Lee, B.-Y. Park, and M. Rho, *Phys. Rev. C* **83**, 025206 (2011).
 - [18] B.-A. Li, L.-W. Chen, and C. M. Ko, *Phys. Rep.* **464**, 113 (2008).
 - [19] B. A. Brown, *Phys. Rev. Lett.* **85**, 5296 (2000).
 - [20] A. Szmagłinski, W. Wojcik, and M. Kutschera, *Acta Phys. Pol. B* **37**, 277 (2006).
 - [21] A. E. L. Dieperink, Y. Dewulf, D. Van Neck, M. Waroquier, and V. Rodin, *Phys. Rev. C* **68**, 064307 (2003).
 - [22] A. W. Steiner, M. Prakash, J. M. Lattimer, and P. J. Ellis, *Phys. Rep.* **411**, 325 (2005).
 - [23] C.-H. Lee, T. T. S. Kuo, G. Q. Li, and G. E. Brown, *Phys. Rev. C* **57**, 3488 (1998).
 - [24] C. J. Horowitz and J. Piekarewicz, *Phys. Rev. Lett.* **86**, 5647 (2001).
 - [25] L.-W. Chen, C. M. Ko, and B.-A. Li, *Phys. Rev. C* **76**, 054316 (2007).
 - [26] Z. H. Li, U. Lombardo, H.-J. Schulze, W. Zuo, L. W. Chen, and H. R. Ma, *Phys. Rev. C* **74**, 047304 (2006).
 - [27] V. R. Pandharipande and V. K. Garde, *Phys. Lett. B* **39**, 608 (1972).
 - [28] B. Friedman and V. R. Pandharipande, *Nucl. Phys. A* **361**, 502 (1981).
 - [29] R. B. Wiringa, V. Fiks, and A. Fabrocini, *Phys. Rev. C* **38**, 1010 (1988).
 - [30] N. Kaiser, S. Fritsch, and W. Weise, *Nucl. Phys. A* **697**, 255 (2002).
 - [31] P. G. Krastev and F. Sammarruca, *Phys. Rev. C* **74**, 025808 (2006).
 - [32] E. Chabanat, J. Meyer, P. Bonche, R. Schaeffer, and P. Haensel, *Nucl. Phys. A* **627**, 710 (1997).
 - [33] J. R. Stone, J. C. Miller, R. Koncewicz, P. D. Stevenson, and M. R. Strayer, *Phys. Rev. C* **68**, 034324 (2003).
 - [34] L.-W. Chen, C. M. Ko, and B.-A. Li, *Phys. Rev. C* **72**, 064309 (2005).
 - [35] J. Decharge and D. Gogny, *Phys. Rev. C* **21**, 1568 (1980).
 - [36] C. B. Das, S. Das Gupta, C. Gale, and B.-A. Li, *Phys. Rev. C* **67**, 034611 (2003).
 - [37] D. T. Khoa, W. von Oertzen, and A. A. Ogloblin, *Nucl. Phys. A* **602**, 98 (1996).
 - [38] D. N. Basu, P. R. Chowdhury, and C. Samanta, *Nucl. Phys. A* **811**, 140 (2008).
 - [39] W. D. Myers and W. J. Swiatecki, *Acta Phys. Pol. B* **26**, 111 (1995).
 - [40] S. Banik and D. Bandyopadhyay, *J. Phys. G* **26**, 1495 (2000).
 - [41] P. R. Chowdhury, D. N. Basu, and C. Samanta, *Phys. Rev. C* **80**, 011305 (2009).
 - [42] C. Xu and B.-A. Li, *Phys. Rev. C* **81**, 064612 (2010).
 - [43] C. Xu, A. Li, and B.-A. Li, [arXiv:1207.1639](https://arxiv.org/abs/1207.1639).
 - [44] Z. Xiao, B.-A. Li, L.-W. Chen, G.-C. Yong, and M. Zhang, *Phys. Rev. Lett.* **102**, 062502 (2009).

- [45] P. Russotto *et al.*, *Phys. Lett. B* **697**, 471 (2011).
- [46] W. Trautmann and H. H. Wolter, *Int. J. Mod. Phys. E* **21**, 1230003 (2012).
- [47] L. F. Roberts, G. Shen, V. Cirigliano, J. A. Pons, S. Reddy, and S. E. Woosley, *Phys. Rev. Lett.* **108**, 061103 (2012).
- [48] É. É. Flanagan and T. Hinderer, *Phys. Rev. D* **77**, 021502 (2008).
- [49] T. Hinderer, *Astrophys. J.* **677**, 1216 (2008).
- [50] T. Binnington and E. Poisson, *Phys. Rev. D* **80**, 084018 (2009).
- [51] T. Damour and A. Nagar, *Phys. Rev. D* **80**, 084035 (2009).
- [52] T. Damour and A. Nagar, *Phys. Rev. D* **81**, 084016 (2010).
- [53] T. Hinderer, B. D. Lackey, R. N. Lang, and J. S. Read, *Phys. Rev. D* **81**, 123016 (2010).
- [54] S. Postnikov, M. Prakash, and J. M. Lattimer, *Phys. Rev. D* **82**, 024016 (2010).
- [55] L. Baiotti, T. Damour, B. Giacomazzo, A. Nagar, and L. Rezzolla, *Phys. Rev. Lett.* **105**, 261101 (2010).
- [56] L. Baiotti, T. Damour, B. Giacomazzo, A. Nagar, and L. Rezzolla, *Phys. Rev. D* **84**, 024017 (2011).
- [57] B. D. Lackey, K. Kyutoku, M. Shibata, P. R. Brady, and J. L. Friedman, *Phys. Rev. D* **85**, 044061 (2012).
- [58] F. Pannarale, L. Rezzolla, F. Ohme, and J. S. Read, *Phys. Rev. D* **84**, 104017 (2011).
- [59] T. Damour, A. Nagar, and L. Villain, *Phys. Rev. D* **85**, 123007 (2012).
- [60] B. D. Serot and J. D. Walecka, *Adv. Nucl. Phys.* **16**, 1 (1986).
- [61] B. D. Serot and J. D. Walecka, *Int. J. Mod. Phys. E* **6**, 515 (1997).
- [62] H. Mueller and B. D. Serot, *Nucl. Phys. A* **606**, 508 (1996).
- [63] B. G. Todd-Rutel and J. Piekarewicz, *Phys. Rev. Lett.* **95**, 122501 (2005).
- [64] B. Liu, V. Greco, V. Baran, M. Colonna, and M. Di Toro, *Phys. Rev. C* **65**, 045201 (2002).
- [65] V. Baran, M. Colonna, V. Greco, and M. Di Toro, *Phys. Rep.* **410**, 335 (2005).
- [66] G. A. Lalazissis, J. König, and P. Ring, *Phys. Rev. C* **55**, 540 (1997).
- [67] G. A. Lalazissis, S. Raman, and P. Ring, *At. Data Nucl. Data Tables* **71**, 1 (1999).
- [68] J. Piekarewicz, *Phys. Rev. C* **76**, 064310 (2007).
- [69] F. J. Fattoyev, C. J. Horowitz, J. Piekarewicz, and G. Shen, *Phys. Rev. C* **82**, 055803 (2010).
- [70] A. Schwenk and C. J. Pethick, *Phys. Rev. Lett.* **95**, 160401 (2005).
- [71] E. N. E. van Dalen and H. Muther, *Phys. Rev. C* **80**, 037303 (2009).
- [72] K. Hebeler and A. Schwenk, *Phys. Rev. C* **82**, 014314 (2010).
- [73] S. Gandolfi, A. Y. Illarionov, S. Fantoni, F. Pederiva, and K. E. Schmidt, *Phys. Rev. Lett.* **101**, 132501 (2008).
- [74] A. Gezerlis and J. Carlson, *Phys. Rev. C* **81**, 025803 (2010).
- [75] I. Vidaña, A. Polls, and A. Ramos, *Phys. Rev. C* **65**, 035804 (2002).
- [76] D. H. Youngblood, H. L. Clark, and Y.-W. Lui, *Phys. Rev. Lett.* **82**, 691 (1999).
- [77] Y.-W. Lui, D. Youngblood, S. Shlomo, X. Chen, Y. Tokimoto *et al.*, *Phys. Rev. C* **83**, 044327 (2011).
- [78] R. Furnstahl, J. J. Rusnak, and B. D. Serot, *Nucl. Phys. A* **632**, 607 (1998).
- [79] A. W. Steiner, J. M. Lattimer, and E. F. Brown, *Astrophys. J.* **722**, 33 (2010).
- [80] L.-W. Chen, C. M. Ko, B.-A. Li, and J. Xu, *Phys. Rev. C* **82**, 024321 (2010).
- [81] L. W. Chen, B. J. Cai, C. M. Ko, B. A. Li, C. Shen, and J. Xu, *Phys. Rev. C* **80**, 014322 (2009).
- [82] E. N. E. van Dalen, C. Fuchs, and A. Faessler, *Phys. Rev. Lett.* **95**, 022302 (2005).
- [83] P. Reinhard, *Rep. Prog. Phys.* **52**, 439 (1989).
- [84] Y. Gambhir, P. Ring, and A. Thimet, *Ann. Phys. (NY)* **198**, 132 (1990).
- [85] A. Bodmer, *Nucl. Phys. A* **526**, 703 (1991).
- [86] S. Ulrych and H. Muther, *Phys. Rev. C* **56**, 1788 (1997).
- [87] R. Xu, Z. Ma, E. N. E. van Dalen, and H. Muther, *Phys. Rev. C* **85**, 034613 (2012).
- [88] M. Jaminon and C. Mahaux, *Phys. Rev. C* **40**, 354 (1989).
- [89] B. G. Todd and J. Piekarewicz, *Phys. Rev. C* **67**, 044317 (2003).
- [90] F. Özel, G. Baym, and T. Güver, *Phys. Rev. D* **82**, 101301 (2010).
- [91] F. Özel, D. Psaltis, R. Narayan, and A. S. Villarreal, *Astrophys. J.* **757**, 55 (2012).
- [92] J. Abadie *et al.* (LIGO Scientific Collaboration, Virgo Collaboration), *Class. Quant. Grav.* **27**, 173001 (2010).